THE JOURNAL OF BIOLOGICAL CHEMISTRY VOL. 291, NO. 48, pp. 25227–25238, November 25, 2016
© 2016 by The American Society for Biochemistry and Molecular Biology, Inc. Published in the U.S.A.

Four-and-a-half LIM Domains 1 (FHL1) Protein Interacts with the Rho Guanine Nucleotide Exchange Factor PLEKHG2/FLJ00018 and Regulates Cell Morphogenesis*

Received for publication, September 20, 2016, and in revised form, October 20, 2016 Published, JBC Papers in Press, October 20, 2016, DOI 10.1074/jbc.M116.759571

Katsuya Sato[‡1], Masashi Kimura[§2], Kazue Sugiyama[‡], Masashi Nishikawa[‡], Yukio Okano[§], Hitoshi Nagaoka[§], Takahiro Nagase[¶], Yukio Kitade[‡‖], and Hiroshi Ueda[‡‖3]

From the [‡]United Graduate School of Drug Discovery and Medical Information Sciences and the [§]Department of Molecular Pathobiochemistry, Gifu University Graduate School of Medicine, Yanagido 1-1, Gifu 501-1193, Japan, the [¶]Kazusa DNA Research Institute, 2-6-7 Kazusa-kamatari, Kisarazu, Chiba 292-0818, Japan, and the [‖]Department of Chemistry and Biomolecular Science, Faculty of Engineering, Gifu University, Yanagido 1-1, Gifu 501-1193, Japan

Edited by Henrik Dohlman

PLEKHG2/FLJ00018 is a Gβγ-dependent guanine nucleotide exchange factor for the small GTPases Rac and Cdc42 and has been shown to mediate the signaling pathways leading to actin cytoskeleton reorganization. Here we showed that the zinc finger domain-containing protein four-and-a-half LIM domains 1 (FHL1) acts as a novel interaction partner of PLEKHG2 by the yeast two-hybrid system. Among the isoforms of FHL1 (*i.e.* FHL1A, FHL1B, and FHL1C), FHL1A and FHL1B interacted with PLEKHG2. We found that there was an FHL1-binding region at amino acids 58–150 of PLEKHG2. The overexpression of FHL1A but not FHL1B enhanced the PLEKHG2-induced serum response element-dependent gene transcription. The co-expression of FHL1A and Gβγ synergistically enhanced the PLEKHG2-induced serum response element-dependent gene transcription. Increased transcription activity was decreased by FHL1A knock-out with the CRISPR/Cas9 system. Compared with PLEKHG2-expressing cells, the number and length of finger-like protrusions were increased in PLEKHG2-, Gβγ-, and FHL1A-expressing cells. Our results provide evidence that FHL1A interacts with PLEKHG2 and regulates cell morphological change through the activity of PLEKHG2.

Cytoskeletal regulation is governed largely by the precise temporal and spatial modulation of the small G-proteins of the Rho family (Rho GTPases), RhoA, Rac, and Cdc42 (1). The Rho GTPases function as molecular switches. They are converted from the GDP-bound inactive form to a GTP-bound active state by a reaction catalyzed by Rho GTPase-specific guanine nucleotide exchange factors (RhoGEFs).[4] RhoGEFs are large multidomain proteins that are tightly regulated to control their function. RhoGEFs can be subdivided into two main subfamilies. First, there are those that possess a Dbl homology (DH) domain that is found in tandem with a pleckstrin homology (PH) domain. This subfamily is currently represented by 70 members in mammalian genomes (2, 3). Second, there are Dock180-related proteins containing the Dock homology region-2 domain (also known as the Docker-ZH2 domain), which form a subfamily of 11 mammalian members (4). The DH domain is responsible for catalytic activity, and the PH domain directs subcellular localization and can modulate the DH domain function.

A number of the DH domain-containing RhoGEFs, including PSD-95/Dlg/ZO-1 (PDZ)-RhoGEF, leukemia-associated RhoGEF, and p115-RhoGEF, have a regulator of G-protein signaling (RGS) domain in addition to a DH domain and PH domain. PDZ-RhoGEF and LARG also have a PDZ domain. These RhoGEFs are regulated by activated $G\alpha_{12/13}$ subunits through their interaction with the RGS domain to activate GDP/GTP exchange activity for RhoA (5–7). In contrast, P-Rex1 and P-Rex2 are regulated by Gβγ subunits and polyphosphoinositide through direct interaction to activate the GDP/GTP exchange activity for Rac (8). We reported that one novel RhoGEF, PLEKHG2/FLJ00018, was activated by direct interaction with Gβγ subunits and regulated cell spreading through the activation of Rac1 and Cdc42 (9). In 2014, we reported that the phosphorylation of PLEKHG2 by Ras/MAPK pathways regulated the morphological change of cells (10). We also reported that the tyrosine phosphorylation of PLEKHG2 by the EphB2/cSrc pathway induced an interaction between PLEKHG2 and PIK3R3 (11). Finally, we demonstrated that PLEKHG2 interacted with β-actin and γ-actin and that both β- and γ-actin acted as negative regulators of PLEKHG2 (12). However, the details underlying the molecular mechanisms of PLEKHG2 activation have yet to be elucidated.

* This study was supported by JSPS KAKENHI Grants 23590073 and 15K07927. The DNA sequence analysis was supported by the Division of Genomic Research at the Life Science Research Center at Gifu University. The authors declare that they have no conflicts of interest with the contents of this article.

[1] Present address: Dept. of Molecular Pathobiochemistry, Gifu University Graduate School of Medicine, Yanagido 1-1, Gifu, 501-1193, Japan.

[2] Present address: Dept. of Cell Signaling, Gifu University Graduate School of Medicine, Yanagido 1-1, Gifu 501-1193, Japan.

[3] To whom correspondence should be addressed: Dept. of Chemistry and Biomolecular Science, Faculty of Engineering, Gifu University, Yanagido, Gifu 501-1193, Japan. Tel.: 81-58-230-7634; Fax: 81-58-230-7604; E-mail: hueda@gifu-u.ac.jp.

[4] The abbreviations used are: RhoGEF, Rho GTPase-specific guanine nucleotide exchange factor; DH, Dbl homology; PH, pleckstrin homology; RGS, regulator of G-protein signaling; aa, amino acid(s); NLS, nuclear localization sequence; mAG, monomeric Azami Green.

In light of the above findings, PLEKHG2 is thought to regulate actin reorganization by Rho through various intercellular signal pathways, including the G protein-coupled receptor pathway. In the present study, using two-hybrid screening, we demonstrated that a zinc finger domain-containing protein, four-and-a-half LIM domains 1 (FHL1), acts as a binding partner of PLEKHG2. Our findings suggested that the binding with FHL1 positively regulated the activity of PLEKHG2 and the morphological changes of cells.

Results

Isolation and Identification of FHL1 as a Binding Partner of PLEKHG2—We previously investigated the binding partners of the N-terminal region of PLEKHG2 (amino acids (aa) 1–465) using yeast two-hybrid screening. Among 128 positive clones, 24 clones showed high homology (>80%) to genes in the database (12). The amino acid sequence of one of the positive clones was identical to aa 111–323 of FHL1B. In vertebrates, there are three FHL1 isoforms: FHL1A, FHL1B, and FHL1C. FHL1A is characterized by an N-terminal half-LIM domain followed by four complete LIM domains. FHL1B has an initial three and one-half N-terminal LIM domains that are identical to those of FHL1A as well as a novel C-terminal sequence including three functional nuclear localization sequences (NLSs) and a nuclear export sequence. FHL1C has an initial two and a half N-terminal LIM domains that are identical to those of FHL1A.

In general, it is thought that LIM domains mediate protein-protein interactions that are critical to cellular processes (13). The prey amino acid sequence contains the sequences of the C-terminal part of the second LIM domain and the third LIM domain of FHL1A and FHL1B (Fig. 1*A*). To demonstrate the interaction of PLEKHG2 with FHL1A or FHL1B in mammalian cells, we co-transfected expression vectors of PLEKHG2 and FHL1A or FHL1B into HEK293 cells. After transfected cells were immunoprecipitated with PLEKHG2, FHL1A and FHL1B were co-immunoprecipitated with PLEKHG2. However, PLEKHG2 bound more strongly with FHL1A than FHL1B in HEK293 cells (Fig. 1*B*). FHL1B has an NLS, and it is thought that FHL1B is located in the nucleus (14). In contrast, PLEKHG2 is thought to act mainly at the cytosol. It seems that the PLEKHG2 cannot gain access to the FHL1B. This might result in a weak binding of these two proteins. Indeed, most of the FHL1B was eliminated as a lysis buffer-insoluble fraction that included insoluble proteins and nuclear proteins (Fig. 1*B*).

Next, to examine whether FHL1A and FHL1B interacted with regions other than aa 1–465 of PLEKHG2, cells were co-transfected with PLEKHG2 ΔNT and FHL1A or FHL1B. PLEKHG2 ΔNT was immunoprecipitated by anti-Myc antibody, and both the FHL1A and FHL1B isoforms were detected in the anti-Myc immunoprecipitate (Fig. 1, *C* and *D*). The level of FHL1A or FHL1B co-immunoprecipitated with PLEKHG2 ΔNT was the same as that co-immunoprecipitated with the PLEKHG2 WT. We suspect that the binding regions may also be present in the ΔNT region of PLEKHG2. The interaction of PLEKHG2 P2 and FHL1 was much stronger than the interaction of the PLEKHG2 WT and FHL1. We and other researchers showed that the C terminus of PLEKHG2 interacted with the N terminus of PLEKHG2 (9, 15). We consider that when PLEKHG2 was activated, the C terminus region of PLEKHG2 opened, and the DH domain at the N terminus region exerted some activity. Perhaps, when PLEKHG2 was activated, PLEKHG2 remained as a stable form in the cells. The fact that PLEKHG2 P2 and PLEKHG2 ΔNT interacted with FHL1 suggests that this interaction might have physiological meaning in mammalian cells.

The FHL1-binding Region of PLEKHG2—To detect the FHL1-binding region of PLEKHG2, we performed co-immunoprecipitation with various deletion mutants of PLEKHG2 (Fig. 2*A*). HEK293 cells were transiently transfected with the deletion mutants of PLEKHG2 and FLAG-tagged FHL1A. As shown in Fig. 2*B*, FHL1A was co-immunoprecipitated with P2 (aa 1–464) and P2ΔN1 (aa 58–464). However, P2ΔN2 (aa 150–464) and P2ΔN3 (aa 283–464) showed little co-immunoprecipitation with FHL1A.

We also examined the C terminus region-deleted mutants of the P2 mutant (Fig. 2*C*). FHL1A was co-immunoprecipitated with P2ΔC1 (aa 1–441), P2ΔC2 (aa 1–355), and P2ΔC3 (aa 1–310). However, PH (aa 283–441) showed little co-immunoprecipitation with FHL1A. These results suggested that the amino acid region 58–150 of PLEKHG2 is an FHL1-binding region in PLEKHG2.

Effect of FHL1 on the PLEKHG2-induced Serum Response Element (SRE)-dependent Gene Transcription in HEK293 Cells—To examine whether the expression of FHL1 influences PLEKHG2 functions in cells, we measured the transcription of an SRE-controlled reporter gene that is known to be induced by Rho family activation (16). Co-expression of the PLEKHG2 WT and FHL1A enhanced PLEKHG2-induced SRE-dependent gene transcription. In contrast, the co-expression of PLEKHG2 with FHL1B was almost not affected (Fig. 3, *A* and *B*). Co-expression of the PLEKHG2 P2 mutant and FHL1A or FHL1B yielded similar results (Fig. 3, *A* and *B*).

As mentioned above, we previously reported that PLEKHG2 is activated by G$\beta\gamma$ to increase SRE-dependent gene transcription through the activation of Rac and Cdc42 (9). To examine whether the expression of FHL1 influences PLEKHG2 functions in the presence of G$\beta\gamma$, the PLEKHG2 WT or P2 and FHL1A or FHL1B with or without G$\beta\gamma$ were co-transfected into cells. Co-expression of PLEKHG2 and G$\beta\gamma$ with FHL1A synergistically enhanced PLEKHG2-induced SRE-dependent gene transcription (Fig. 4, *A*–C). In contrast, the co-expression of FHL1B was almost unaffected (Fig. 4, *A*–C). Co-expression of the PLEKHG2 P2 mutant and FHL1A or FHL1B with or without G$\beta\gamma$ yielded similar results (Fig. 4, *D*–*F*). These results suggested that FHL1A acts as a positive regulator of PLEKHG2 in mammalian cells.

The Interaction of PLEKHG2 with FHL1 and G$\beta\gamma$—To examine why PLEKHG2-induced SRE-dependent gene transcription is synergistically enhanced in PLEKHG2-, FHL1A-, and G$\beta\gamma$-expressing cells, we investigated the interaction of PLEKHG2 with FHL1 and G$\beta\gamma$ in the cells by co-immunoprecipitation experiments. PLEKHG2 was immunoprecipitated by anti-Myc antibody, and FHL1A (Fig. 5*A*, *lane 2*) and Gβ (Fig. 5*B*, *lane 2*) were detected in the anti-Myc immunoprecipitate. When we transfected G$\beta\gamma$ in addition to PLEKHG2 and FHL1A, G$\beta\gamma$ interacted with PLEKHG2 (Fig. 5*A*, *lane 3*). However, compar-

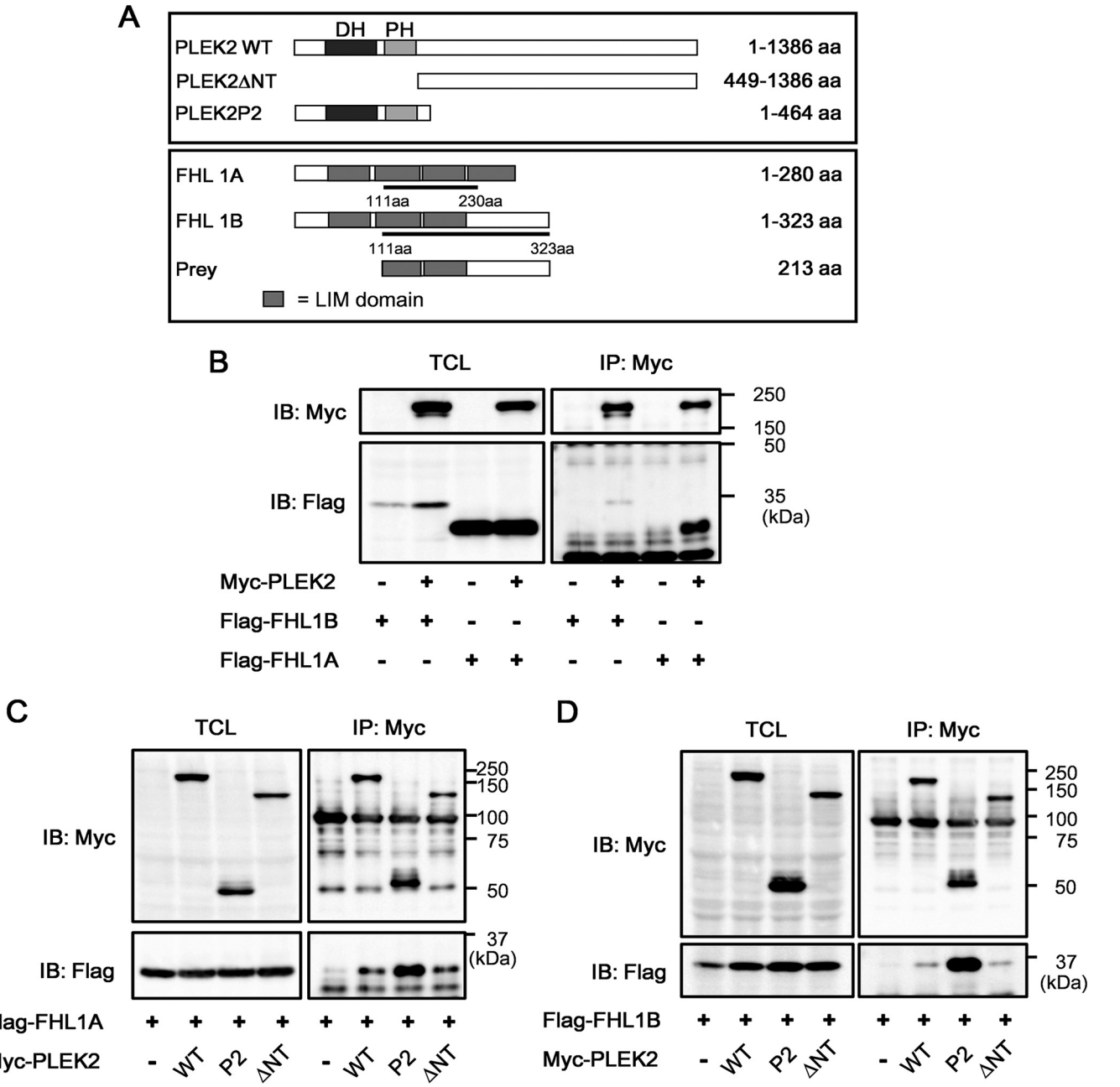

FIGURE 1. **PLEKHG2 bound with both FHL1A and FHL1B.** *A*, schematic diagram of PLEKHG2 mutants and FHL1. *Prey*, yeast two-hybrid prey construct. PLEK2 ΔNT and P2 constructs code amino acid residues 449–1386 and 1–464 of PLEKHG2, respectively. *Underlining* and *amino acid numbers* indicate the sequences detected by yeast two-hybrid screening. *B–D*, HEK293 cells were co-transfected with PLEKHG2 or PLEKHG2 mutants and FHL1A or FHL1B, as indicated. Cells were lysed 24 h after transfection, and PLEKHG2 was immunoprecipitated with anti-Myc antibody. Precipitated proteins were separated by SDS-PAGE and immunoblotted with anti-Myc antibody (for PLEKHG2) and anti-FLAG antibody (for FHL1). *PLEK2*, PLEKHG2; *TCL*, total cell lysate; *IP*, immunoprecipitation; *IB*, immunoblotting.

ing the results in *lanes 2* and *3* of Fig. 5*A*, it can be seen that the levels of the PLEKHG2 and FHL1A interaction were not altered by G$\beta\gamma$ expression, and *vice versa* (Fig. 5*B*, *lanes 2* and *3*). In addition, FLAG-tagged-FHL1A was immunoprecipitated by anti-FLAG antibody as a reverse immunoprecipitation, and PLEKHG2 was detected in the immunoprecipitant by anti-FLAG antibody (Fig. 5*C*, *lanes 3* and *4*). Moreover, FLAG-tagged-FHL1A was immunoprecipitated by anti-FLAG antibody, and G$\beta\gamma$ was detected in the anti-FLAG immunoprecipitant (Fig. 5*C*, *lanes 1* and *2*). These results suggest that PLEKHG2, FHL1A, and G$\beta\gamma$ form a complex in the co-expressing cells. This complex formation appeared to be related to the synergistic enhancement of SRE-dependent gene transcription. We recently reported that the interaction of PLEKHG2 with non-muscle actin attenuated PLEKHG2-induced SRE-dependent gene transcription (12). To examine the effect of non-muscle actin on the enhancement of PLEKHG2-induced SRE-dependent gene transcription by the co-expression of FHL1A, PLEKHG2, FHL1A, and β-actin were co-expressed in the cells. The co-expression of β-actin with PLEKHG2 and FHL1A attenuated the PLEKHG2-induced SRE-dependent gene transcription (Fig. 6, *A* and *B*). These results suggest that β-actin

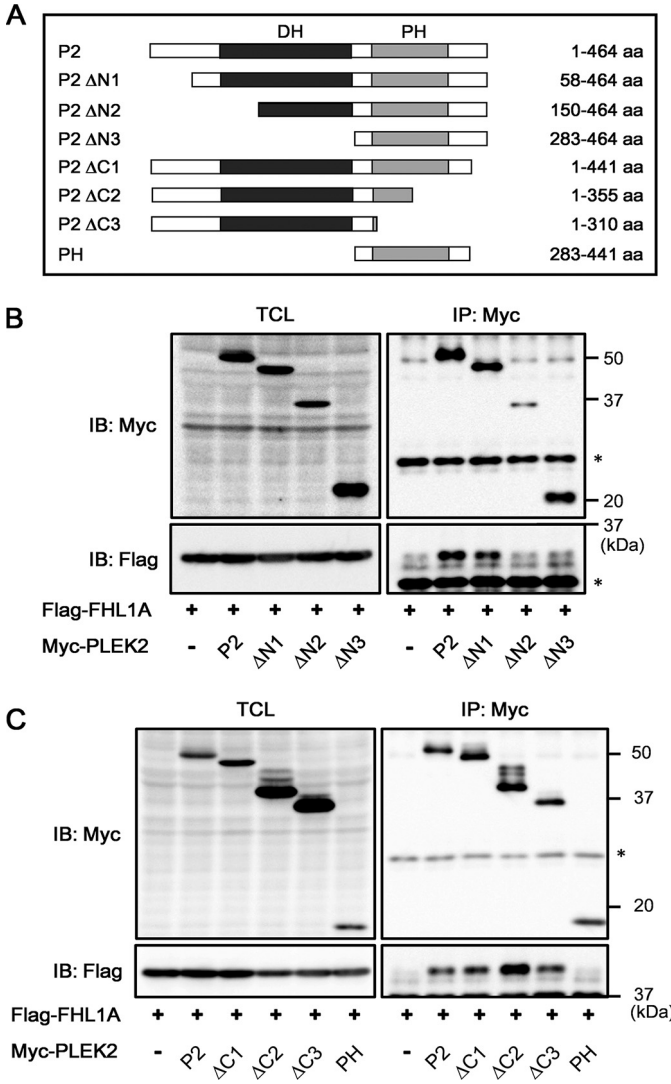

FIGURE 2. **Amino acids 58–150 of PLEKHG2 bound to FHL1A.** *A*, schematic diagram of PLEKHG2 P2 mutants. The PLEK2 P2, P2ΔN1, P2ΔN2, P2ΔN3, P2ΔC1, P2ΔC2, P2ΔC3, and PH constructs code amino acid residues 1–464, 58–464, 150–464, 283–464, 1–441, 1–355, 1–310, and 283–441 of PLEKHG2, respectively. *B* and *C*, HEK293 cells were co-transfected with PLEKHG2 P2 or PLEKHG2 P2 mutants and FHL1A, as indicated. Cells were lysed 24 h after transfection, and PLEKHG2 was immunoprecipitated with anti-Myc antibody. Precipitated proteins were separated by SDS-PAGE and immunoblotted with anti-Myc antibody (for PLEKHG2) and anti-FLAG antibody (for FHL1). *PLEK2*, PLEKHG2; *TCL*, total cell lysate; *IP*, immunoprecipitation; *IB*, immunoblotting. *, immunoglobulins precipitated by immunoprecipitation.

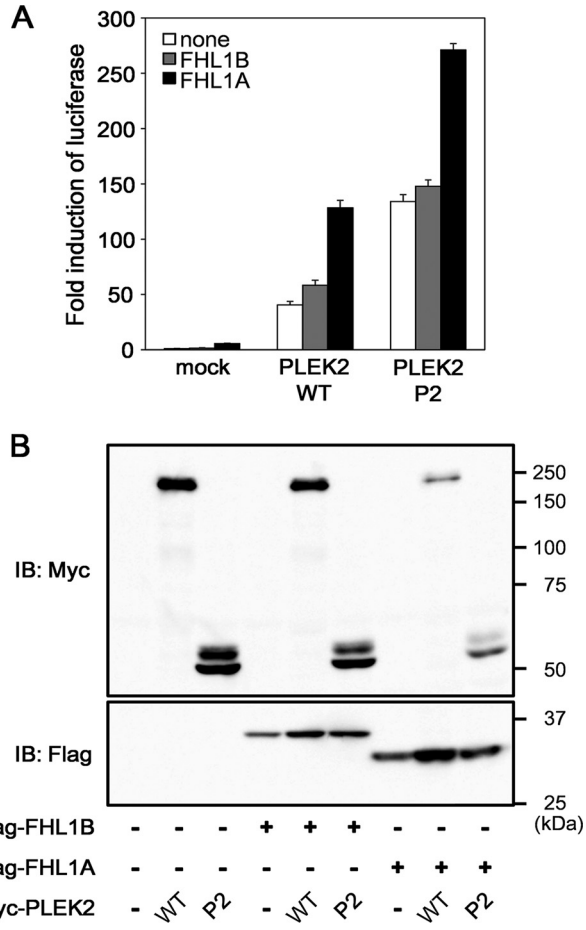

FIGURE 3. **FHL1A enhanced PLEKHG2-induced SRE-dependent gene transcription.** *A*, HEK293 cells were co-transfected with pSRE.L-luciferase, pRL-SV40, PLEKHG2, PLEKHG2 P2, FHL1A, and FHL1B, as indicated. The cells were lysed 24 h after transfection, and the effect of FHL1 protein on PLEKHG2-induced transcription was analyzed by a luciferase reporter gene assay. The experiment was performed in triplicate, and the values are the means ± S.D. (*error bars*). The data shown are representative of three independent experiments. *B*, HEK293 cells were co-transfected with PLEKHG2, PLEKHG2 P2, FHL1A, and FHL1B, as indicated. Cells were lysed 24 h after transfection, and the lysates were separated by SDS-PAGE and immunoblotted with anti-Myc antibody (for PLEKHG2) and anti-FLAG antibody (for FHL1). *PLEK2*, PLEKHG2. *IB*, immunoblotting.

interacted with a region different from the FHL1-binding region of PLEKHG2 and that this interaction inhibited the function of PLEKHG2.

Effect of FHL1 on the Gβγ- and PLEKHG2-induced SRE-dependent Gene Transcription in HEK293 Cells—To confirm that FHL1 and PLEKHG2 interacted and functioned in the cells, we used genome-editing tools and generated FHL1-knock-out cells. Anti-FHL1 antibody could detect both the exogenous FHL1A and endogenous FHL1A in HEK293 cells (Fig. 7*A*). Although anti-FHL1 antibody could detect transfected FHL1B, it failed to detect endogenous FHL1B in HEK293 cells. For this reason, it was thought that HEK293 cells express endogenous FHL1A but not FHL1B (Fig. 7*A*). We also checked the cells of a mouse neuroblastoma cell line, Neuro-2a. However, we could not detect endogenous FHL1A and FHL1B in these cells. Using mouse tissue, we confirmed that this antibody is capable of detecting FHL1B and FHL1A (data not shown). Next, we tried to knock out endogenous FHL1 protein in HEK293 cells. We constructed two CRISPR/Cas9 plasmids at FHL1 exons 2 and 3 to delete this region (Fig. 7*B*). After introducing CRISPR/Cas9 plasmids, the cells were single cell-sorted. Cloned cells were checked by PCR analysis (Fig. 7*C*). From the immunoblot analysis, we confirmed that the knock-out cells did not express the FHL1A protein (Fig. 7*D*).

To the best of our knowledge, no PLEKHG2 antibody with a capacity for immunoprecipitation has been identified. To examine whether endogenous FHL1A interacts with PLEKHG2, we transfected Myc-tagged PLEKHG2 into wild type cells and knock-out cells. In the wild type cells, endogenous FHL1 was co-precipitated with Myc-tagged PLEKHG2, and this interaction did not appear in knock-out cells (Fig. 8*A*). This result suggested that PLEKHG2 might interact with FHL1

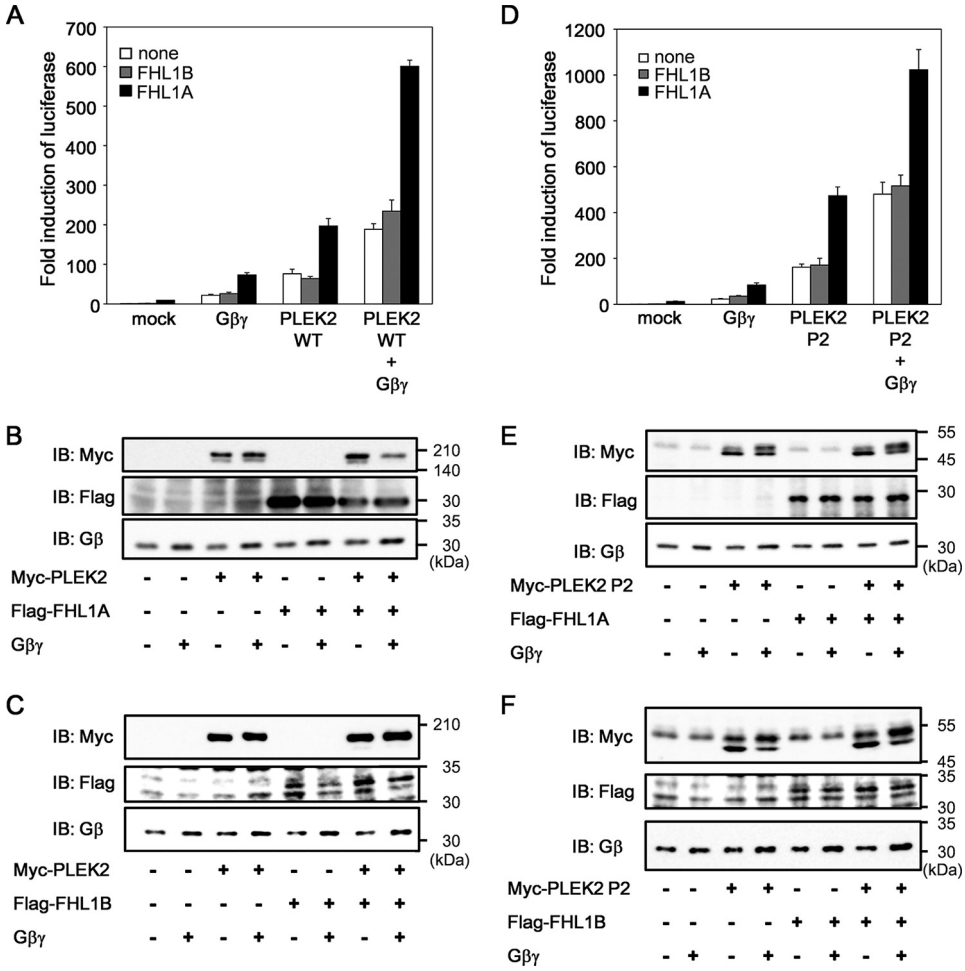

FIGURE 4. **Gβγ enhanced FHL1A- and PLEKHG2-induced SRE-dependent gene transcription.** *A* and *D*, HEK293 cells were co-transfected with pSRE.L-luciferase, pRL-SV40, PLEKHG2, PLEKHG2 P2, FHL1A, FHL1B, and Gβγ, as indicated. The cells were lysed 24 h after transfection, and the effect of FHL1 protein on PLEKHG2-induced transcription was analyzed by a luciferase reporter gene assay. The experiment was performed in triplicate, and the values are the means ± S.D. (*error bars*). The data shown are representative of three independent experiments. *B*, *C*, *E*, and *F*, HEK293 cells were co-transfected with PLEKHG2, PLEKHG2 P2, FHL1A, FHL1B, and Gβγ, as indicated. Cells were lysed 24 h after transfection, and the lysates were separated by SDS-PAGE and immunoblotted with anti-Myc antibody (for PLEKHG2) and anti-FLAG antibody (for FHL1). *PLEK2*, PLEKHG2. *IB*, immunoblotting.

in HEK293 cells. Next, we performed an SRE-dependent gene transcription assay to reveal the effect of FHL1 on the PLEKHG2 signaling. Consistent with the other results, Gβγ enhanced PLEKHG2-induced SRE-dependent gene transcription. In contrast, the level of enhancement of SRE-dependent gene transcription was much lower in Gβγ- and PLEKHG2-transfected FHL1-knock-out cells (Fig. 8*B*). Enforced expression of FHL1 in FHL1-knock-out cells rescued the Gβγ- and PLEKHG2-induced SRE-dependent gene transcription (Fig. 8, *C* and *D*). Although it is still unclear whether FHL1 functions by interacting directly with PLEKHG2 and Gβγ, this result indicates that FHL1 plays an important role in Gβγ- and PLEKHG2-induced signaling.

Effect of FHL1A and FHL1B on the PLEKHG2-related Morphological Changes in Neuro-2a Cells—We subjected a fetal brain cDNA library to yeast two-hybrid screening to find the binding partner of PLEKHG2, and we used a mouse neuroblastoma cell line, Neuro-2a, to examine the cellular localization and cell morphological changes of PLEKHG2 and its binding partners to determine their functional meanings. First, we confirmed that FHL1A interacted with PLEKHG2 in Neuro-2a cells (Fig. 9*A*) and that FHL1A enhanced PLEKHG2-induced SRE-dependent gene transcription (Fig. 9, *B* and *C*). FHL1B interacted with PLEKHG2 in Neuro-2a cells (Fig. 9*D*). However, FHL1B failed to activate PLEKHG2-induced SRE-dependent gene transcription (Fig. 9, *E* and *F*). These results are consistent with the results we obtained using HEK293 cells. From these observations, we speculate that FHL1A activates PLEKHG2 in Neuro-2a cells, using the same system as in HEK293 cells.

Next, to reveal the effect of PLEKHG2 and FHL1A on the cell morphology, we co-transfected mAG-tagged PLEKHG2, FLAG-tagged FHL1A, FLAG-tagged FHL1B, and Gβγ. FHL1B was localized at the center of the cell. It appeared not to co-localize with PLEKHG2 (Fig. 10*B*). When co-expressing FHL1B and PLEKHG2, the cells were slightly spread. When the cells co-expressed FHL1B, PLEKHG2, and Gβγ, the spreading effect was enhanced. However, based on our observation that the spread cells were also present among cells that expressed PLEKHG2 or PLEKHG2 and Gβγ (Fig. 10*A*), it appears that this effect was not caused by FHL1B. On the other hand, when we co-transfected with PLEKHG2, FHL1A, and Gβγ, FHL1A was

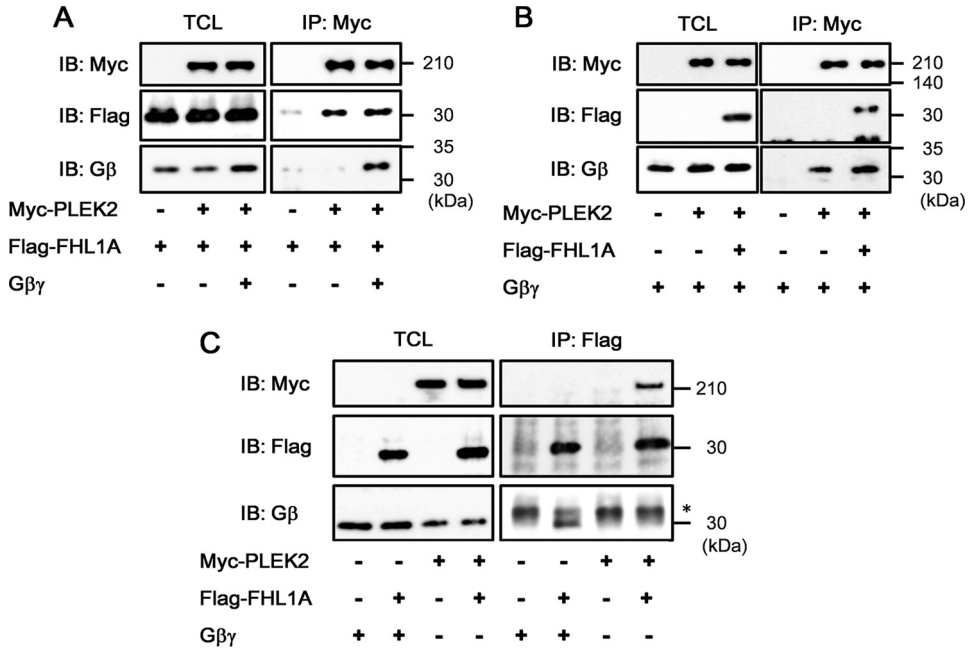

FIGURE 5. **FHL1A, G$\beta\gamma$, and PLEKHG2 formed a ternary complex.** *A–C*, HEK293 cells were co-transfected with Myc-tagged PLEKHG2, FLAG-tagged FHL1A, and G$\beta\gamma$, as indicated. Cells were lysed 24 h after transfection, and PLEKHG2 (*A* and *B*) or FHL1A (*C*) was immunoprecipitated with anti-Myc or anti-FLAG antibody. Precipitated proteins were separated by SDS-PAGE and immunoblotted with anti-Myc antibody (for PLEKHG2), anti-FLAG antibody (for FHL1), or Gβ antibody (for Gβ). *PLEK2*, PLEKHG2; *TCL*, total cell lysate; *IP*, immunoprecipitation. *, immunoglobulins precipitated from immunoprecipitation. *IB*, immunoblotting.

stained throughout the cell. In addition, neurite-like shapes were observed in the PLEKHG2-, FHL1A-, and G$\beta\gamma$-transfected cells (Fig. 10*C*). We performed further analysis to confirm that the neurite-like structure of the FHL1A-, PLEKHG2-, and G$\beta\gamma$-transfected cells was truly different from the cell morphology of the PLEKHG2- and G$\beta\gamma$-transfected cells. Using ImageJ software, we measured the length and number of cell protrusions (Fig. 10, *D* and *E*). In the cells expressing PLEKHG2, G$\beta\gamma$, and FHL1A, both the length and number of cell protrusions were increased from the PLEKHG2- and G$\beta\gamma$-expressing cells. Because we were unable to detect endogenous FHL1 expression in Neuro-2a cells, we could not examine the relationship between the signal enhancement and this morphological change. However, this result supports the notion that the expressions of FLH1A, PLEKHG2, and G$\beta\gamma$ can promote the morphological change.

Discussion

The results of this study revealed that a zinc finger LIM domain-containing protein, FHL1, interacted with PLEKHG2. FHL1s are divided into mainly three isoforms: FHL1A, FHL1B, and FHL1C. The results of the yeast two-hybrid screening suggested that PLEKHG2 interacted with LIM2 and LIM3. Although both FHL1A and FHL1B have LIM2 and LIM3, PLEKHG2 was bound more strongly with FHL1A. FHL1B has an NLS. It seems that most of the FHL1B protein was localized in the nucleus. For this reason, we speculate that it is difficult for PLEKHG2 to gain access to the FHL1B. This is consistent with our finding that FHL1B was stained at the center of the cells, whereas PLEKHG2 was stained at the cytosol in Neuro-2a cells.

It was previously reported that FHL1B was localized at the cytosol during the G_2 phase of the cell cycle. FHL1B interacts with protein phosphatase 2A catalytic subunit β during this phase to shuttle between the nucleus and cytoplasm (17). It is possible that PLEKHG2 interacts with FHL1B only at a specific time point in the cell cycle and may play one or more specific roles. Further analysis is necessary.

The binding region of FHL1 and PLEKHG2 exists within aa 58–150 of PLEKHG2. In this paper, we used various deletion mutants to analyze the binding region. One of the mutants, PLEKHG2 ΔN2, is missing parts of the DH domain. We cannot exclude the possibility that this mutant generates a misfolded protein. However, in our previous paper (9), we used another DH domain deletion mutant and found that this mutant still functioned as a G$\beta\gamma$-binding protein (PLEKHG2 p5, aa 1–108; PLEKHG2 p6, aa 1–149; PLEKHG2 p7, aa 1–134). From this observation, we considered that the PLEKHG2 ΔN2 mutant still maintains its conformation, at least in terms of protein-protein interaction. The FHL1A-binding region of PLEKHG2 was identical to the G$\beta\gamma$-binding region of PLEKHG2 that we reported previously (9). Indeed, our present findings suggested that PLEKHG2, G$\beta\gamma$, and FHL1A may form a ternary complex. As can be seen in Fig. 5, *A* and *B*, the amount of FHL1A and G$\beta\gamma$ interacting with PLEKHG2 did not decrease in the cells transfected with PLEKHG2, FHL1, and G$\beta\gamma$. On the other hand, FHL1 interacted with G$\beta\gamma$ (see Fig. 5*C*). We could not analyze the binding region of FHL1 that interacted with G$\beta\gamma$ in detail; thus, further analysis will be needed to unravel the binding mechanisms. In contrast, the β-actin-binding region exists within aa 150–283 of PLEKHG2. The interaction of β-actin and PLEKHG2 has been shown to inhibit PLEKHG2-induced SRE-dependent gene transcription (12). In light of these observations, aa 58–158 of PLEKHG2 may play an important role in the

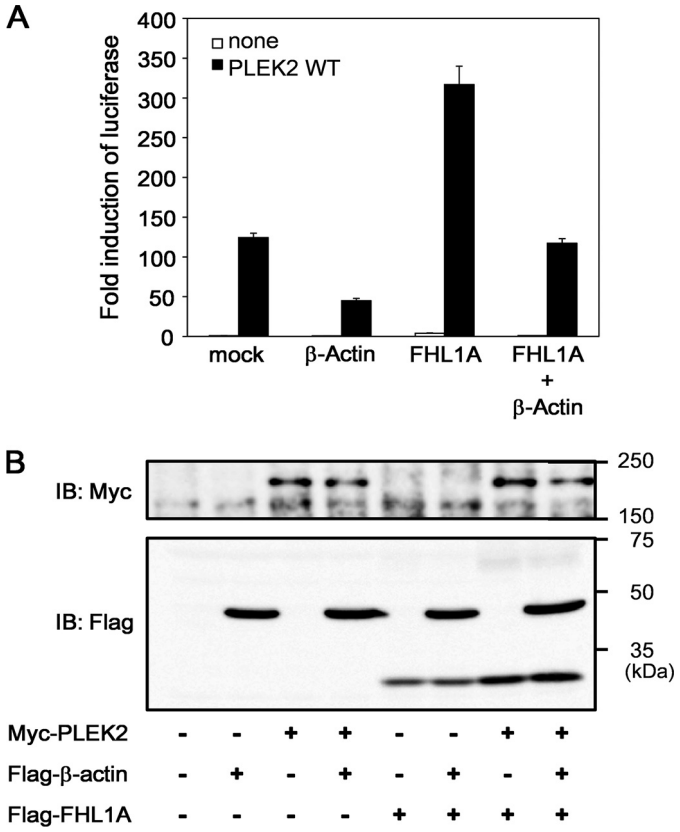

FIGURE 6. ***β*-Actin inhibited the FHL1A-activated, PLEKHG2-induced SRE-dependent gene transcription.** *A*, HEK293 cells were co-transfected with pSRE.L-luciferase, pRL-SV40, PLEKHG2, FHL1A, and *β*-actin, as indicated. Cells were lysed 24 h after transfection, and the effect of FHL1 protein on PLEKHG2-induced transcription was analyzed by a luciferase reporter gene assay. The experiment was performed in triplicate, and the values are the means ± S.D. (*error bars*) The data shown are representative of three independent experiments. *B*, HEK293 cells were co-transfected with PLEKHG2, FHL1A, and *β*-actin, as indicated. Cells were lysed 24 h after transfection, and the lysates were separated by SDS-PAGE and immunoblotted with anti-Myc antibody (for PLEKHG2) or anti-FLAG antibody (for FHL1 and *β*-actin). *PLEK2*, PLEKHG2. *IB*, immunoblotting.

activity of PLEKHG2. Recently, we and other researchers suggested that the C terminus of PLEKHG2 might interact with the N terminus of PLEKHG2, and this interaction could impose a constraint on the normal DH domain function by masking the access of the Rho GTPase (9, 15). It has been hypothesized that, when PLEKHG2 is activated, the interaction between the C and N termini is canceled, and the DH domain functions as a guanine nucleotide exchange factor for the Rho protein. The binding of FHL1A and G$\beta\gamma$ to PLEKHG2 might help to prevent the intramolecular interaction of PLEKHG2. However, the details of such inhibition are unclear, and further analysis will be needed to determine the novel functional domain of PLEKHG2.

PLEKHG2-induced SRE-dependent gene transcription was activated by the expression of FHL1A. Moreover, the co-expression of FHL1A and G$\beta\gamma$ synergistically enhanced the PLEKHG2-induced SRE-dependent gene transcription. In this study, we used CRISPR/Cas9 to deplete FHL1 expression in HEK293 cells. In the FHL1-knock-out cells, the interaction between FHL1 and PLEKHG2 was not observed. Fig. 8 shows the results of our signaling experiments using FHL1-knock-out cells. FHL1 reduced the G$\beta\gamma$-stimulated PLEKHG2-induced SRE-dependent gene transcription. Although it is still unclear whether FHL1 functions via a direct interaction with PLEKHG2 and G$\beta\gamma$, we think these observations suggest that FHL1 is involved in the G$\beta\gamma$-stimulated PLEKHG2 activation.

The cellular functions of other FHL proteins (*i.e.* Act, FHL2, and FHL3) were recently reported. These proteins act as co-activators of androgen receptor (18–20). The activation of Rho plays an especially important role in the nuclear localization of FHL2 (20). Moreover, FHL2 interacts with phosphorylated ERK2 to inhibit the transcription of ELK-1 and GATA4 in the nucleus (21). However, there is much evidence that FHL2 acts as a distinct compartment of the cytosol. For example, it has been reported that FHL2 localized to the focal adhesion or interacted with integrin, a cell adhesion molecule (22, 23). As shown in these studies, the FHL protein interacted with a wide variety of cytoplasmic and nuclear proteins and localized to a specific compartment. We showed that the morphology of Neuro-2a cells was changed upon transfection with PLEKHG2, G$\beta\gamma$, and FHL1A. Neurite-like protrusions were increased in these cells, and FHL1A and PLEKHG2 appeared to be co-localized at the protrusions. FHL1A may retain or promote PLEKHG2 and G$\beta\gamma$ to the edge of the neurite-like protrusions. Taken together with the fact that PLEKHG2-, G$\beta\gamma$-, and FHL1A-expressing cells increased the SRE-dependent gene transcription, this finding suggests that the protrusion was caused by Cdc42 activation. However, further analyses (including live-imaging analyses) will be needed to confirm that this phenotype is caused by filopodial type projections and/or retraction. We also tried to knock out FHL1A and FHL1B in Neuro-2a cells. However, Neuro-2a cells did not express endogenous FHL1A or FHL1B (see Fig. 7*A*). For this reason, we could not examine the relation between signaling and morphology. Further studies will be needed to investigate this subject as well.

As we described above, we performed yeast two-hybrid screening using a fetal brain cDNA library as a candidate for the binding partner of PLEKHG2. There has been a report describing that FHL1B protein expression was observed in the brain (24). In the present study, PLEKHG2 was co-immunoprecipitated with FHL1A and FHL1B in both HEK293 and Neuro-2a cells. PLEKHG2 interacted with the LIM2 and LIM3, which is a common sequence of FHL1A and FHL1B. FHL1 and PLEKHG2 may play important roles in the brain. FHL1A is expressed in tissues other than brain tissue, and its function is linked to specific diseases. For example, FHL1A is highly expressed in skeletal muscle, and its mutation causes myopathy or Duchenne muscular dystrophy (25, 26). Further understanding of the interaction with FHL1 and PLEKHG2 may help to clarify the clinical conditions of not only the brain but also other body tissues.

Experimental Procedures

Plasmids—Human FHL1A and FHL1B were cloned by PCR amplification from human brain cDNA (QUICK-Clone™ cDNA, Clontech, Mountain View, CA). Amplified fragments were digested by using Flexi Enzyme Mix (Promega, Madison, WI) and ligated into pF5A-FLAG-neo vector. pF5A-CMV-neo-Gβ_1 and pF5A-CMV-neo-Gγ_2 were described previously (27).

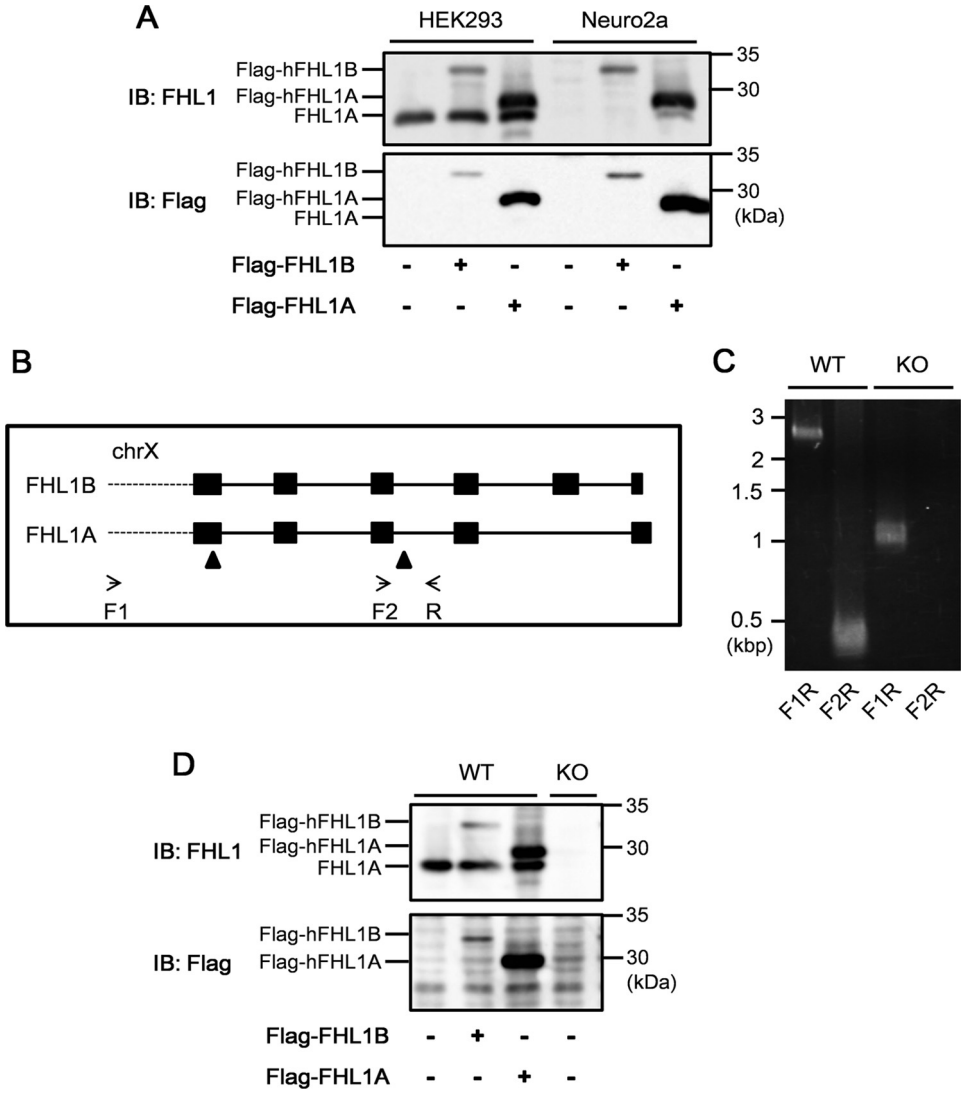

FIGURE 7. **Establishment of FHL1-deleted cell lines.** *A*, HEK293 cells or Neuro-2a cells were co-transfected with FHL1B and FHL1A, as indicated. Cells were lysed 24 h after transfection, and the lysates were separated by SDS-PAGE and immunoblotted with anti-FHL1 antibody (for exogenous and endogenous FHL1) and anti-FLAG antibody (for exogenous FHL1). *Flag-h-FHL1B*, FLAG-tagged human FHL1B; *Flag-h-FHL1A*, FLAG-tagged human FHL1A; *FHL1A*, endogenous FHL1A. *B*, schematic diagram of the genome around the FHL1-coding region. Two genomic RNAs (*arrowheads*) were introduced to HEK293 cells. The genomic RNAs were designed to delete exons 2 and 3, which included the functional domain of the protein. Primers (*arrows*) were used for genotyping. Three primers were designed to amplify the inside of the deletion region. *C*, sorted cells were lysed, and the genomic DNA was isolated. Then PCR analysis was performed with isolated genomic DNA. *F1R* and *F2R*, the primer set shown in *B*. *D*, wild type or FHL1 protein-knock-out HEK293 cells were co-transfected with FHL1B and FHL1A, as indicated. Cells were lysed 24 h after transfection, and the lysate was separated by SDS-PAGE and immunoblotted with anti-FHL1 antibody (for exogenous and endogenous FHL1) or anti-FLAG antibody (for exogenous FHL1). *Flag-h-FHL1B*, FLAG-tagged human FHL1B; *Flag-h-FHL1A*, FLAG-tagged human FHL1A; *FHL1A*, endogenous FHL1A. *IB*, immunoblotting.

The pFN21A-Myc-PLEKHG2 wild type, various expression vectors of PLEKHG2 mutants, and pFN21K-mAG-PLEKHG2 coding the monomeric green fluorescent protein, Azami Green (mAG), were described previously (12). The CRISPR/Cas9 expression vector pSpCas9(BB)-2A-Puro (PX459) was a gift from Feng Zhang (AddGene plasmid 48139). This vector was linearized by a restriction enzyme, BbsI. Two sets of synthesized oligonucleotides primers (the set 5′-CACCGACCTTGGAGTCCGCACCGAT-3′ and 5′-AAACATCGGTGCGGACTCCAAGGTC-3′ and the set 5′-CACCGAGATGAGGAGATCGTGGATT-3′ and 5′-AAACAATCCACGATCTCCTCATCTC-3′) were annealed and ligated into linearized vector with each other. All constructs were verified by sequencing before use. The pSRE.L-luciferase reporter plasmid was purchased from Stratagene (Santa Clara, CA), and pRL-SV40 was purchased from Nippon Gene (Tokyo, Japan).

Yeast Two-hybrid Screening—The details of the yeast two-hybrid screening have been described previously (12). Briefly, a Gal4 DNA-binding domain fusion protein, pGBKT7-PLEKHG2 (aa 1–465), was used as a bait vector. Bait plasmids were transformed into the yeast strain Y187. A pretransformed human fetal brain cDNA-Gal4 activation domain fusion library in pGADT7 was used to identify interacting proteins (Clontech). Prey plasmids were pretransformed into the yeast strain Y2H Gold. Positive clones were first selected on synthetic dropout medium in the absence of Leu and Trp. The colonies obtained were spotted onto synthetic dropout medium in the absence of adenine, His, Leu, and Trp. The interaction was fur-

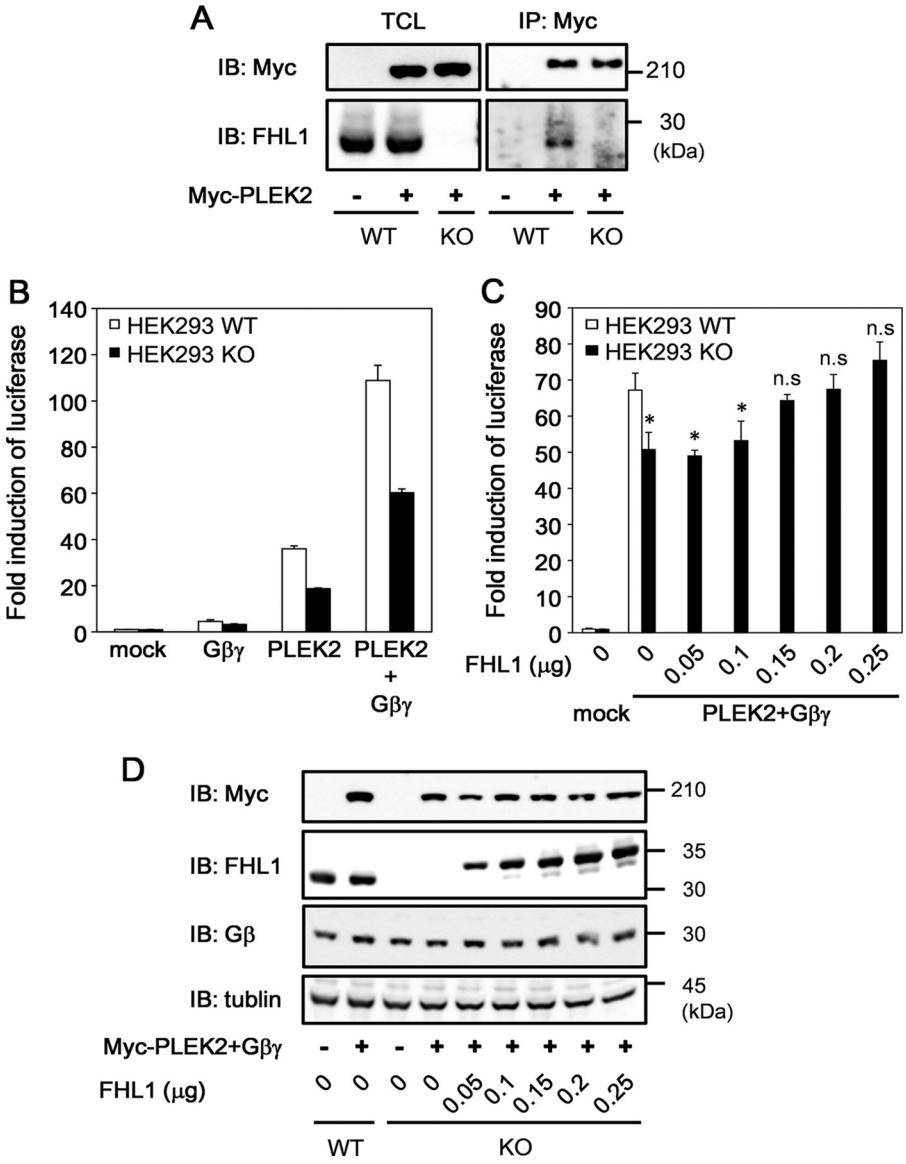

FIGURE 8. **Effect of FHL1 on Gβγ- and PLEKHG2-induced SRE-dependent gene transcription.** *A*, wild type or FHL1-knock-out HEK293 cells were transfected with Myc-tagged PLEKHG2, as indicated. Cells were lysed 24 h after transfection, and the lysates were separated by SDS-PAGE and immunoblotted with anti-Myc antibody (for PLEKHG2) and anti-FHL1 antibody (for FHL1). *PLEK2*, PLEKHG2. *B* and *C*, wild type or FHL1-knock-out HEK293 cells were co-transfected with pSRE.L-luciferase, pRL-SV40, PLEKHG2, Gβγ, and FHL1A, as indicated. Cells were lysed 24 h after transfection, and the SRE-dependent gene transcription was analyzed by a luciferase reporter gene assay. The experiment was performed in triplicate, and the values are the means ± S.D. (*error bars*). The data shown are representative of three independent experiments. *, $p < 0.05$ compared with PLEKHG2- and Gβγ-expressing HEK293 WT cells. *n.s.*, not significant. *D*, wild type or FHL1-knock-out HEK293 cells were co-transfected with PLEKHG2, Gβγ, and FHL1A, as indicated. Cells were lysed 24 h after transfection, and the lysates were separated by SDS-PAGE and immunoblotted with anti-Myc antibody (for PLEKHG2), anti-FLAG antibody (for FHL1), Gβ antibody (for Gβ), or anti-tubulin-γ antibody (for γ-tubulin). *PLEK2*, PLEKHG2. *IB*, immunoblotting.

ther confirmed by co-transforming the library plasmid of interest and pGBKT7-PLEKHG2 (aa 1–465) into Y2H Gold.

Cell Culture and Transfection—HEK293 and Neuro-2a cells were grown in DMEM supplemented with 10% fetal bovine serum at 37 °C. Transient transfection was performed using Lipofectamine2000 reagent according to the manufacturer's instructions (Life Technologies, Inc.). Cells were transfected with DNA for 6–9 h and then washed with serum-free DMEM and incubated for 16–18 h in DMEM.

Generation of FHL1-knock-out Cells—Two CRISPR/Cas9 constructs and pEGFP-N2 were introduced into HEK293 cells as described above. Cells were resuspended in 5 mM EDTA containing PBS. Then cells were single cell-sorted onto 96-well plates (SH-800, SONY, Tokyo, Japan). Expanded cells were lysed in tail digestion buffer (0.1 mM Tris-HCl, 5 mM EDTA, 0.2% SDS, 2 mM NaCl, and 0.4 mg/ml protease K). Lysed cells were heated for 3 h at 55 °C, and then whole genome DNA was isolated by chloroform extraction and ethanol precipitation. The genome DNA that was isolated from cloned cells was checked by PCR analysis as described under "Results."

Assay of SRE-dependent Gene Transcription—Cells seeded in 24-well plates were co-transfected with the indicated expression plasmids together with the pSRE.L-luciferase reporter plasmid and the pRL-SV40 control reporter plasmids. After transfection, cells were washed once with ice-cold PBS and lysed with passive lysis buffer. Luciferase activities were deter-

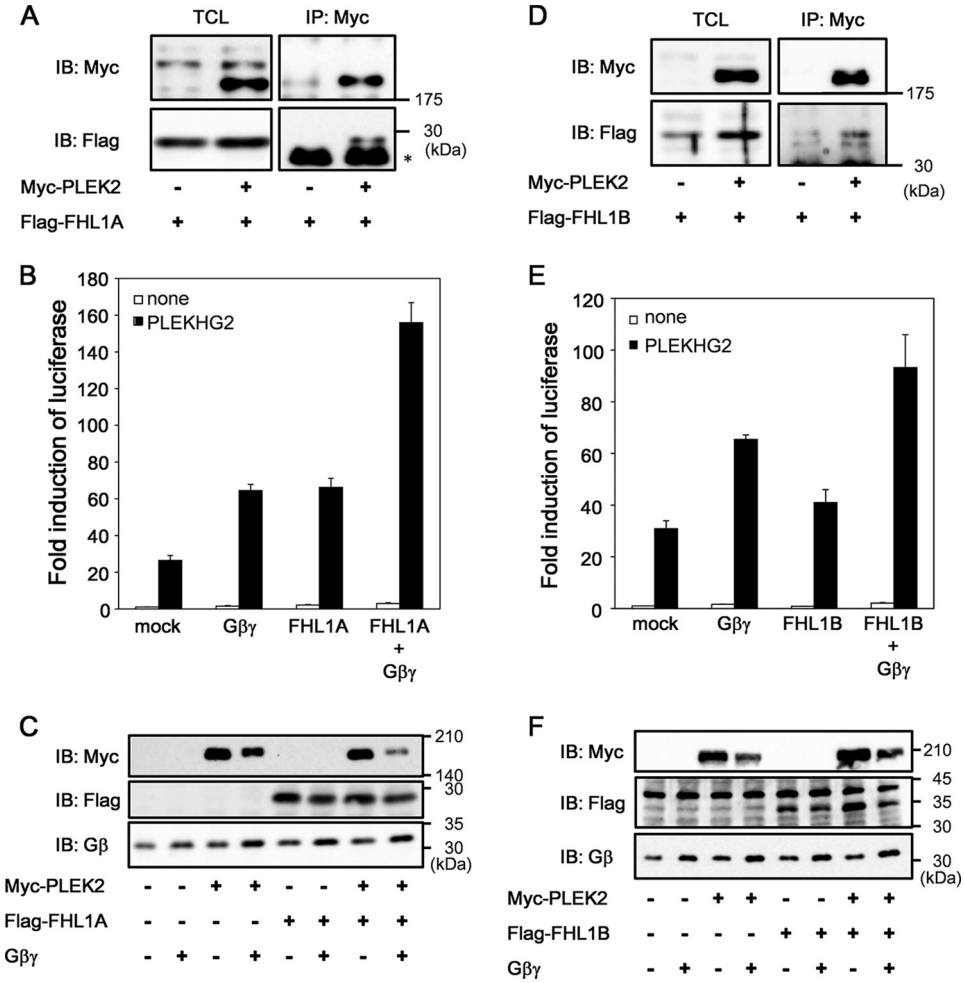

FIGURE 9. **PLEKHG2 and FLH1A were co-localized in Neuro-2a cells and regulated cell morphogenesis.** *A* and *D*, Neuro-2a cells were co-transfected with Myc-tagged PLEKHG2 and FLAG-tagged FHL1A or FHL1B, as indicated. Cells were lysed 24 h after transfection, and PLEKHG2 was immunoprecipitated with anti-Myc antibody. Precipitated proteins were separated by SDS-PAGE and immunoblotted with anti-Myc antibody (for PLEKHG2) or anti-FLAG antibody (for FHL1). *B* and *E*, Neuro-2a cells were co-transfected with pSRE.L-luciferase, pRL-SV40, PLEKHG2, FHL1A, FHL1B, and G$\beta\gamma$, as indicated. Cells were lysed 24 h after transfection, and the effect of FHL1 protein on PLEKHG2-induced transcription was analyzed by a luciferase reporter gene assay. The experiment was performed in triplicate, and the values are the means ± S.D. (*error bars*). The data shown are representative of three independent experiments. *C* and *F*, Neuro-2a cells were co-transfected with PLEKHG2, FHL1A, FHL1B, and G$\beta\gamma$, as indicated. Cells were lysed 24 h after transfection, and the lysate was separated by SDS-PAGE and immunoblotted with anti-Myc antibody (for PLEKHG2) and anti-FLAG antibody (for FHL1). *PLEK2*, PLEKHG2; *TCL*, total cell lysate; *IP*, immunoprecipitation. *IB*, immunoblotting. *, immunoglobulins precipitated from immunoprecipitation.

mined by using a Dual-Luciferase Reporter (DLR^{TM}) assay system (Promega). The activity of the experimental reporter was normalized against the activity of the control vector.

Immunoprecipitation—Transfected cells seeded in 6-cm dishes were washed once with ice-cold PBS and lysed with lysis buffer (50 mM Tris-HCl, pH 7.5, 100 mM NaCl, 0.1 mM EDTA, 1 mM Na_3VO_4, 0.5% Nonidet P-40, phosphatase inhibitor solution, and protease inhibitor solution). The lysates were centrifuged to remove residue (13,200 rpm for 10 min). Clear lysates were incubated with 1.0 μg of anti-Myc IgG or 1.0 μg of anti-FLAG IgG for 2 h at 4 °C and then mixed with protein G-agarose (EMD Milipore, Billerica, MA) or protein A-Sepharose (GE Healthcare, Buckinghamshire, UK) for 1 h at 4 °C. The beads were washed three times with washing buffer (50 mM Tris-HCl, pH 7.5, 100 mM NaCl, 0.1 mM EDTA, 1 mM Na_3VO_4, 0.1% Nonidet P-40, phosphatase inhibitor solution, and protease inhibitor solution). Bound proteins were eluted with sample buffer. For Gβ co-immunoprecipitation and endogenous FHL1 precipitation, the protein-bound beads were incubated with 0.4 mg/ml c-Myc peptide (Wako, Osaka, Japan) overnight at 4 °C. Then the eluted proteins were denatured by sample buffer. Equal amounts of samples were resolved by 7.5, 10, or 10–20% gradient SDS-PAGE. 10–20% gradient SDS-polyacrylamide gel was from Gellex International Co., Ltd. (Tokyo, Japan). The transferred PVDF membrane was tested by immunoblot analysis as described below.

Immunoblot Analysis—Transfected cells seeded in 35-mm dishes were washed once with ice-cold PBS and lysed with 1% (w/v) SDS in distilled water. The protein concentration of each lysate was quantified using a bicinchoninic acid protein assay kit (Thermo Scientific, Rockford, IL), with BSA as the standard. The same amounts of protein were subjected to 7.5, 10, or 10–20% gradient SDS-PAGE. The transferred PVDF membrane was blocked by 3% skim milk (Morinaga Milk Industry, Tokyo) or 5% BSA (Equitech-bio, Kerrville, TX). For the detection of Myc tag, FLAG tag, β-actin, and FHL1, we used mouse anti-Myc IgG (Wako), mouse anti-FLAG IgG (Wako), mouse anti-β-actin IgG (MBL, Nagoya, Japan), mouse anti-FHL1 IgG

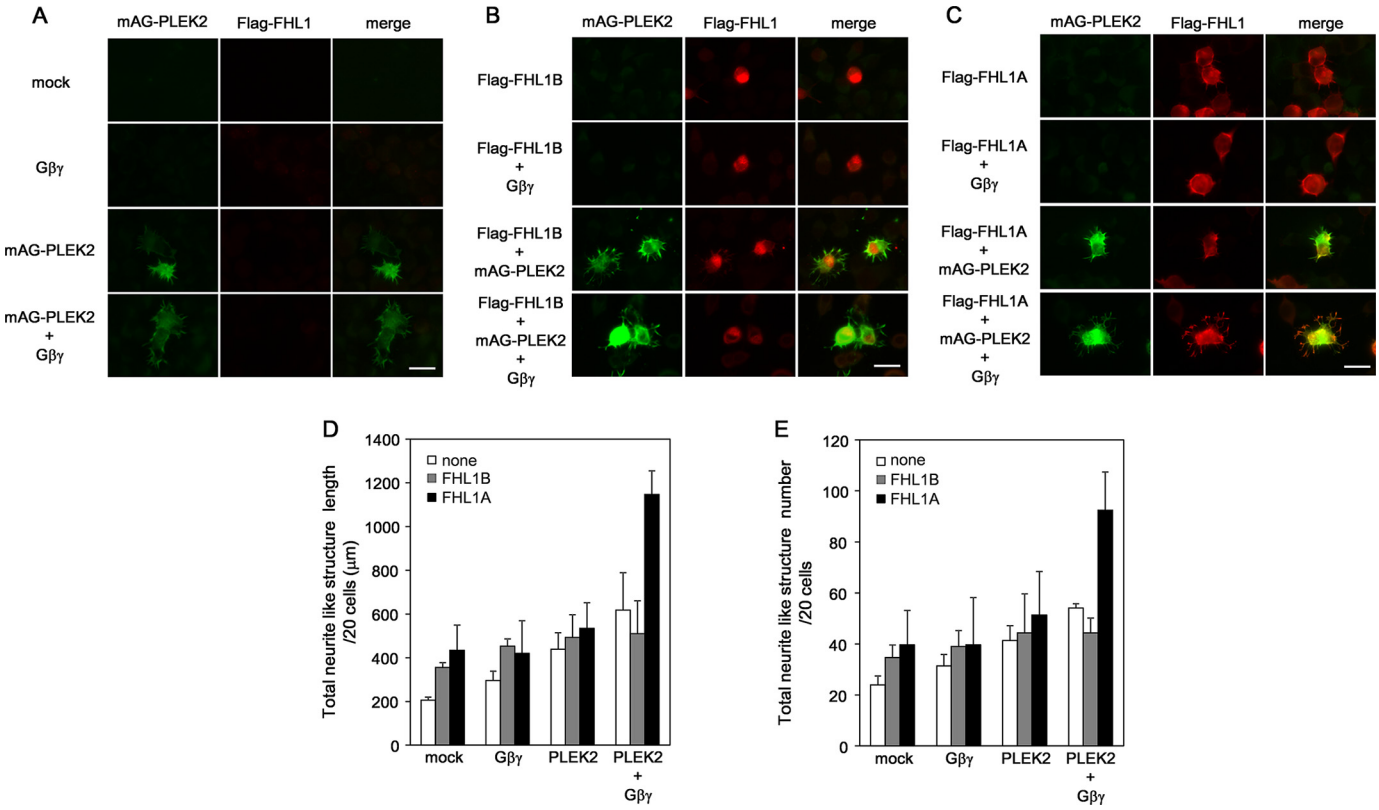

FIGURE 10. **PLEKHG2 and FLH1A were co-localized in Neuro-2a cells and regulated cell morphogenesis.** *A–C*, Neuro-2a cells were co-transfected with mAG-tagged PLEKHG2, FLAG-tagged FHL1A, FLAG-tagged FHL1A, and G$\beta\gamma$, as indicated. After transfection, the cells were fixed and stained with mouse anti-FLAG IgG. The cells were then stained with Alexa Fluor 568-conjugated goat anti-mouse IgG. *Scale bar*, 40 μm. *mAG-PLEK2*, mAG-tagged PLEKHG2. *D* and *E*, Neuro-2a cells were co-transfected with Myc-tagged PLEKHG2, FLAG-tagged FHL1A, FLAG-tagged FHL1A, and G$\beta\gamma$, as indicated. In addition to these plasmids, cells were co-transfected with the expression vector for mAG. After transfection, cells were fixed by 4% paraformaldehyde. At least four fluorescence images were taken from random fields. Total cell protrusion length (*D*) and total cell protrusion number of 20 cells were measured by ImageJ software in each sample. Experiments were repeated multiple times, and the means ± S.D. values (*error bars*) are shown.

(Abcam, Cambridge, MA), and rabbit anti-tubulin-γ IgG (BioLegend, San Diego, CA), respectively. Rabbit anti-Gβ antibody was prepared as described in a previous study and used for the detection of Gβ (9). To detect Myc tag, FLAG tag, β-actin, and FHL1, we used HRP-conjugated anti-mouse IgG as a secondary antibody (MBL). For the detection of Gβ and γ-tubulin, we used HRP-conjugated anti-rabbit IgG as a secondary antibody (MBL). Visualization of HRP-labeled proteins was performed using enzyme-linked chemiluminescence (GE Healthcare or PerkinElmer Life Sciences) and an LAS-4000 mini luminescent image analyzer (GE Healthcare).

Immunofluorescence Analysis—Transfected cells cultured on coverslips were washed once with ice-cold PBS and fixed with 4% paraformaldehyde for 30 min. Fixed cells were permeabilized with 0.1% Triton X-100 in PBS and washed four times with PBS. The cells were then blocked with 10% goat serum in PBS for 1 h. Next, the cells were washed with PBS and incubated with the anti-FLAG antibody and subsequently with secondary antibodies labeled with Alexa Fluor 568 (Life Technologies). The coverslips were then mounted with Perma Fluor. Fluorescence images were acquired using a fluorescence microscope (BZ-9000, Keyence, Tokyo, Japan).

Quantification of Cell Protrusions—Transfected cells cultured on coverslips were washed with ice-cold PBS and fixed with 4% paraformaldehyde for 30 min. The fixed cells were washed four times with PBS. The coverslips were then mounted with Perma Fluor. Four fluorescence images were taken from random fields. The total length of the neurite-like structures of 20 cells and the number of protrusions were analyzed by ImageJ software.

Statistical Analysis—Data are expressed as the means ± S.D. of values from at least three independent experiments. The significance of group differences was analyzed by Student's *t* test. A p value of <0.05 was considered significant.

Author Contributions—K. S., M. K., Y. O., H. N., T. N., Y. K., and H. U. designed the experiments; K. S., M. K., and K. S. carried out the experiments; K. S., M. N., Y. O., H. N., T. N., Y. K., and H. U. carried out the statistical analyses; K. S., K. S., H. N., T. N., Y. K., and H. U. wrote the manuscript.

Acknowledgments—We thank Yoshiko Kurokawa, Ayumi Watanabe, Mayumi Sumi, and Dr. Sigeo Takashima for technical assistance.

References

1. Hall, A. (1998) Rho GTPases and the actin cytoskeleton. *Science* **279,** 509–514
2. Rossman, K. L., Der, C. J., and Sondek, J. (2005) GEF means go: turning on RHO GTPases with guanine nucleotide-exchange factors. *Nat. Rev. Mol. Cell Biol.* **6,** 167–180
3. Zheng, Y. (2001) Dbl family guanine nucleotide exchange factors. *Trends Biochem. Sci.* **26,** 724–732

4. Meller, N., Merlot, S., and Guda, C. (2005) CZH proteins: a new family of Rho-GEFs. *J. Cell Sci.* **118,** 4937–4946
5. Fukuhara, S., Murga, C., Zohar, M., Igishi, T., and Gutkind, J. S. (1999) A novel PDZ domain containing guanine nucleotide exchange factor links heterotrimeric G proteins to Rho. *J. Biol. Chem.* **274,** 5868–5879
6. Fukuhara, S., Chikumi, H., and Gutkind, J. S. (2000) Leukemia-associated Rho guanine nucleotide exchange factor (LARG) links heterotrimeric G proteins of the G_{12} family to Rho. *FEBS Lett.* **485,** 183–188
7. Hart, M. J., Jiang, X., Kozasa, T., Roscoe, W., Singer, W. D., Gilman, A. G., Sternweis, P. C., and Bollag, G. (1998) Direct stimulation of the guanine nucleotide exchange activity of p115 RhoGEF by $G\alpha_{13}$. *Science* **280,** 2112–2114
8. Welch, H. C., Coadwell, W. J., Ellson, C. D., Ferguson, G. J., Andrews, S. R., Erdjument-Bromage, H., Tempst, P., Hawkins, P. T., and Stephens, L. R. (2002) P-Rex1, a PtdIns(3,4,5)P3- and $G\beta\gamma$-regulated guanine-nucleotide exchange factor for Rac. *Cell* **108,** 809–821
9. Ueda, H., Nagae, R., Kozawa, M., Morishita, R., Kimura, S., Nagase, T., Ohara, O., Yoshida, S., and Asano, T. (2008) Heterotrimeric G protein $\beta\gamma$ subunits stimulate FLJ00018, a guanine nucleotide exchange factor for Rac1 and Cdc42. *J. Biol. Chem.* **283,** 1946–1953
10. Sato, K., Sugiyama, T., Nagase, T., Kitade, Y., and Ueda, H. (2014) Threonine 680 phosphorylation of FLJ00018/PLEKHG2, a Rho family-specific guanine nucleotide exchange factor, by epidermal growth factor receptor signaling regulates cell morphology of Neuro-2a cells. *J. Biol. Chem.* **289,** 10045–10056
11. Sato, K., Suzuki, T., Yamaguchi, Y., Kitade, Y., Nagase, T., and Ueda, H. (2014) PLEKHG2/FLJ00018, a Rho family-specific guanine nucleotide exchange factor, is tyrosine phosphorylated via the EphB2/cSrc signaling pathway. *Cell. Signal.* **26,** 691–696
12. Sato, K., Handa, H., Kimura, M., Okano, Y., Nagaoka, H., Nagase, T., Sugiyama, T., Kitade, Y., and Ueda, H. (2013) Identification of a Rho family specific guanine nucleotide exchange factor, FLJ00018, as a novel actin-binding protein. *Cell. Signal.* **25,** 41–49
13. Kadrmas, J. L., and Beckerle, M. C. (2004) The LIM domain: from the cytoskeleton to the nucleus. *Nat. Rev. Mol. Cell Biol.* **5,** 920–931
14. Brown, S., McGrath, M. J., Ooms, L. M., Gurung, R., Maimone, M. M., and Mitchell, C. A. (1999) Characterization of two isoforms of the skeletal muscle LIM protein 1, SLIM1: localization of SLIM1 at focal adhesions and the isoform slimmer in the nucleus of myoblasts and cytoplasm of myotubes suggests distinct roles in the cytoskeleton and in nuclear-cytoplasmic communication. *J. Biol. Chem.* **274,** 27083–27091
15. Runne, C., and Chen, S. (2013) PLEKHG2 promotes heterotrimeric G protein $\beta\gamma$-stimulated lymphocyte migration via Rac and Cdc42 activation and actin polymerization. *Mol. Cell Biol.* **33,** 4294–4307
16. Hill, C. S., Wynne, J., and Treisman, R. (1995) The Rho family GTPases RhoA, Rac1, and CDC42Hs regulate transcriptional activation by SRF. *Cell* **81,** 1159–1170
17. Wong, C. H., Fung, Y. W., Ng, E. K., Lee, S. M., Waye, M. M., and Tsui, S. K. (2010) LIM domain protein FHL1B interacts with PP2A catalytic β subunit: a novel cell cycle regulatory pathway. *FEBS Lett.* **584,** 4511–4516
18. Fimia, G. M., De Cesare, D., and Sassone-Corsi, P. (2000) A family of LIM-only transcriptional coactivators: tissue-specific expression and selective activation of CREB and CREM. *Mol. Cell Biol.* **20,** 8613–8622
19. Müller, J. M., Isele, U., Metzger, E., Rempel, A., Moser, M., Pscherer, A., Breyer, T., Holubarsch, C., Buettner, R., and Schüle, R. (2000) FHL2, a novel tissue-specific coactivator of the androgen receptor. *EMBO J.* **19,** 359–369
20. Müller, J. M., Metzger, E., Greschik, H., Bosserhoff, A. K., Mercep, L., Buettner, R., and Schüle, R. (2002) The transcriptional coactivator FHL2 transmits Rho signals from the cell membrane into the nucleus. *EMBO J.* **21,** 736–748
21. Purcell, N. H., Darwis, D., Bueno, O. F., Müller, J. M., Schüle, R., and Molkentin, J. D. (2004) Extracellular signal-regulated kinase 2 interacts with and is negatively regulated by the LIM-only protein FHL2 in cardiomyocytes. *Mol. Cell Biol.* **24,** 1081–1095
22. Wixler, V., Geerts, D., Laplantine, E., Westhoff, D., Smyth, N., Aumailley, M., Sonnenberg, A., and Paulsson, M. (2000) The LIM-only protein DRAL/FHL2 binds to the cytoplasmic domain of several α and β integrin chains and is recruited to adhesion complexes. *J. Biol. Chem.* **275,** 33669–33678
23. Li, H. Y., Kotaka, M., Kostin, S., Lee, S. M., Kok, L. D., Chan, K. K., Tsui, S. K., Schaper, J., Zimmermann, R., Lee, C. Y., Fung, K. P., and Waye, M. M. (2001) Translocation of a human focal adhesion LIM-only protein, FHL2, during myofibrillogenesis and identification of LIM2 as the principal determinants of FHL2 focal adhesion localization. *Cell Motil. Cytoskeleton* **48,** 11–23
24. Lee, S. M., Li, H. Y., Ng, E. K., Or, S. M., Chan, K. K., Kotaka, M., Chim, S. S., Tsui, S. K., Waye, M. M., Fung, K. P., and Lee, C. Y. (1999) Characterization of a brain-specific nuclear LIM domain protein (FHL1B) which is an alternatively spliced variant of FHL1. *Gene* **237,** 253–263
25. Schessl, J., Taratuto, A. L., Sewry, C., Battini, R., Chin, S. S., Maiti, B., Dubrovsky, A. L., Erro, M. G., Espada, G., Robertella, M., Saccoliti, M., Olmos, P., Bridges, L. R., Standring, P., Hu, Y., *et al.* (2009) Clinical, histological and genetic characterization of reducing body myopathy caused by mutations in FHL1. *Brain* **132,** 452–464
26. Pen, A. E., Nyegaard, M., Fang, M., Jiang, H., Christensen, R., Mølgaard, H., Andersen, H., Ulhøi, B. P., Østergaard, J. R., Vaeth, S., Sommerlund, M., de Brouwer, A. P., Zhang, X., and Jensen, U. B. (2015) A novel single nucleotide splice site mutation in FHL1 confirms an Emery-Dreifuss plus phenotype with pulmonary artery hypoplasia and facial dysmorphology. *Eur. J. Med. Genet.* **58,** 222–229
27. Nagae, R., Sato, K., Yasui, Y., Banno, Y., Nagase, T., and Ueda, H. (2011) G_s and G_q signalings regulate hPEM-2-induced cell responses in Neuro-2a cells. *Biochem. Biophys. Res. Commun.* **415,** 168–173